3. Alyea EP, Kim HT, Ho V, Cutler C, DeAngelo DJ, Stone R, Ritz J, Antin JH, Soiffer RJ. Impact of conditioning regimen intensity on outcome of allogeneic hematopoietic cell transplantation for advanced acute myelogenous leukemia and myelodysplastic syndrome. *Biol Blood Marrow Transplant* 2006;**12**:1047–55.
4. Giralt S, Estey E, Albitar M, *et al.* Engraftment of allogeneic hematopoietic progenitor cells with purine analog-containing chemotherapy: harnessing graft-versus-leukemia without myeloablative therapy. *Blood* 1997;**89**:4531–6.
5. Slavin S, Nagler A, Naparstek E, *et al.* Nonmyeloablative stem cell transplantation and cell therapy as an alternative to conventional bone marrow transplantation with lethal cytoreduction for the treatment of malignant and nonmalignant hematologic diseases. *Blood* 1998;**91**:756–63.
6. Martino R, Iacobelli S, Brand R, *et al.* Retrospective comparison of reduced-intensity conditioning and conventional high-dose conditioning for allogeneic hematopoietic stem cell transplantation using HLA-identical sibling donors in myelodysplastic syndromes. *Blood* 2006;**108**:836–46.
7. Bennett JM, Catovsky D, Daniel MT, Flandrin G, Galton DA, Gralnick HR, Sultan C. Proposals for the classification of the myelodysplastic syndromes. *Br J Haematol* 1982;**51**:189–99.
8. Greenberg P, Cox C, LeBeau MM, *et al.* International scoring system for evaluating prognosis in myelodysplastic syndromes. *Blood* 1997;**89**:2079–88.
9. Przepiorka D, Weisdorf D, Martin P, Klingemann HG, Beatty P, Hows J, Thomas ED. 1994 consensus conference on acute GVHD grading. *Bone Marrow Transplant* 1995;**15**:825–8.
10. Klein JP, Rizzo JD, Zhang MJ, Keiding N. Statistical methods for the analysis and presentation of the results of bone marrow transplants. Part I: unadjusted analysis. *Bone Marrow Transplant* 2001;**28**:909–15.
11. Klein JP, Rizzo JD, Zhang MJ, Keiding N. Statistical methods for the analysis and presentation of the results of bone marrow transplants. Part 2: regression modeling. *Bone Marrow Transplant* 2001;**28**:1001–11.
12. Baron F, Maris MB, Sandmaier BM, *et al.* Graft-versus-tumor effects after allogeneic hematopoietic cell transplantation with nonmyeloablative conditioning. *J Clin Oncol* 2005;**23**: 1993–2003.
13. Prentice RL, Kalbfleisch JD, Peterson AV Jr, Flournoy N, Farewell VT, Breslow NE. The analysis of failure times in the presence of competing risks. *Biometrics* 1978;**34**: 541–54.
14. Horowitz MM, Gale RP, Sondel PM, *et al.* Graft-versus-leukemia reactions after bone marrow transplantation. *Blood* 1990;**75**:555–62.
15. Sullivan KM, Weiden PL, Storb R, *et al.* Influence of acute and chronic graft-versus-host disease on relapse and survival after bone marrow transplantation from HLA-identical siblings as treatment of acute and chronic leukemia. *Blood* 1989;**73**:1720–8.
16. Valcarcel D, Martino R, Caballero D, *et al.* Sustained remissions of high-risk acute myeloid leukemia and myelodysplastic syndrome after reduced-intensity conditioning allogeneic hematopoietic transplantation: chronic graft-versus-host disease is the strongest factor improving survival. *J Clin Oncol* 2008;**26**:577–84.
17. Blaise D, Kuentz M, Fortanier C, *et al.* Randomized trial of bone marrow versus lenograstim-primed blood cell allogeneic transplantation in patients with early-stage leukemia: a report from the Societe Francaise de Greffe de Moelle. *J Clin Oncol* 2000;**18**:537–46.
18. Bensinger WI, Martin PJ, Storer B, *et al.* Transplantation of bone marrow as compared with peripheral-blood cells from HLA-identical relatives in patients with hematologic cancers. *N Engl J Med* 2001;**344**:175–81.
19. Couban S, Simpson DR, Barnett MJ, *et al.* A randomized multicenter comparison of bone marrow and peripheral blood in recipients of matched sibling allogeneic transplants for myeloid malignancies. *Blood* 2002;**100**:1525–31.
20. Finke J, Bethge WA, Schmoor C, *et al.* Standard graft-versus-host disease prophylaxis with or without anti-T-cell globulin in haematopoietic cell transplantation from matched unrelated donors: a randomised, open-label, multicentre phase 3 trial. *Lancet Oncol* 2009;**10**:855–64.
21. Bacigalupo A, Lamparelli T, Bruzzi P, *et al.* Antithymocyte globulin for graft-versus-host disease prophylaxis in transplants from unrelated donors: 2 randomized studies from Gruppo Italiano Trapianti Midollo Osseo (GITMO). *Blood* 2001;**98**:2942–7.
22. Socie G, Schmoor C, Bethge WA, *et al.* Chronic graft-versus-host disease: long-term results from a randomized trial on graft-versus-host disease prophylaxis with or without anti-T-cell globulin ATG-Fresenius. *Blood* 2011;**117**: 6375–82.
23. Fenaux P, Mufti GJ, Hellstrom-Lindberg E, *et al.* Efficacy of azacitidine compared with that of conventional care regimens in the treatment of higher-risk myelodysplastic syndromes: a randomised, open-label, phase III study. *Lancet Oncol* 2009;**10**:223–32.
24. Fenaux P, Mufti GJ, Hellstrom-Lindberg E, *et al.* Azacitidine prolongs overall survival compared with conventional care regimens in elderly patients with low bone marrow blast count acute myeloid leukemia. *J Clin Oncol* 2010;**28**:562–9.
25. de Lima M, Giralt S, Thall PF, de Padua Silva L, Jones RB, Komanduri K, Braun TM, Nguyen HQ, Champlin R, Garcia-Manero G. Maintenance therapy with low-dose azacitidine after allogeneic hematopoietic stem cell transplantation for recurrent acute myelogenous leukemia or myelodysplastic syndrome: a dose and schedule finding study. *Cancer* 2010;**116**:5420–31.
26. Platzbecker U, Wermke M, Radke J, *et al.* Azacitidine for treatment of imminent relapse in MDS or AML patients after allogeneic HSCT: results of the RELAZA trial. *Leukemia* 2012;**26**:381–9.
27. Jabbour E, Giralt S, Kantarjian H, Garcia-Manero G, Jagasia M, Kebriaei P, de Padua L, Shpall EJ, Champlin R, de Lima M. Low-dose azacitidine after allogeneic stem cell transplantation for acute leukemia. *Cancer* 2009;**115**:1899–905.

28. Pinto A, Attadia V, Fusco A, Ferrara F, Spada OA, Di Fiore PP. 5-Aza-2′-deoxycytidine induces terminal differentiation of leukemic blasts from patients with acute myeloid leukemias. *Blood* 1984;**64**:922–9.
29. Pinto A, Maio M, Attadia V, Zappacosta S, Cimino R. Modulation of HLA-DR antigens expression in human myeloid leukaemia cells by cytarabine and 5-aza-2′-deoxycytidine. *Lancet* 1984;**2**:867–8.
30. Momparler RL, Bouchard J, Samson J. Induction of differentiation and inhibition of DNA methylation in HL-60 myeloid leukemic cells by 5-AZA-2′-deoxycytidine. *Leuk Res* 1985;**9**:1361–6.
31. Kanda Y, Izutsu K, Hirai H, *et al.* Effect of graft-versus-host disease on the outcome of bone marrow transplantation from an HLA-identical sibling donor using GVHD prophylaxis with cyclosporin A and methotrexate. *Leukemia* 2004;**18**:1013–9.
32. Shimoni A, Hardan I, Shem-Tov N, Yeshurun M, Yerushalmi R, Avigdor A, Ben-Bassat I, Nagler A. Allogeneic hematopoietic stem-cell transplantation in AML and MDS using myeloablative versus reduced-intensity conditioning: the role of dose intensity. *Leukemia* 2006;**20**:322–8.
33. Lim Z, Brand R, Martino R, *et al.* Allogeneic hematopoietic stem-cell transplantation for patients 50 years or older with myelodysplastic syndromes or secondary acute myeloid leukemia. *J Clin Oncol* 2010;**28**:405–11.
34. Khabori MA, El-Emary M, Xu W, Guyatt G, Galal A, Kuruvilla J, Lipton J, Messner H, Gupta V. Impact of intensity of conditioning therapy in patients aged 40–60 years with AML/myelodysplastic syndrome undergoing allogeneic transplantation. *Bone Marrow Transplant* 2011;**46**:516–22.
35. Scott BL, Sandmaier BM, Storer B, Maris MB, Sorror ML, Maloney DG, Chauncey TR, Storb R, Deeg HJ. Myeloablative vs nonmyeloablative allogeneic transplantation for patients with myelodysplastic syndrome or acute myelogenous leukemia with multilineage dysplasia: a retrospective analysis. *Leukemia* 2006;**20**:128–35.
36. Kuendgen A, Strupp C, Aivado M, Hildebrandt B, Haas R, Gattermann N, Germing U. Myelodysplastic syndromes in patients younger than age 50. *J Clin Oncol* 2006;**24**:5358–65.
37. Sorror ML, Sandmaier BM, Storer BE, Maris MB, Baron F, Maloney DG, Scott BL, Deeg HJ, Appelbaum FR, Storb R. Comorbidity and disease status based risk stratification of outcomes among patients with acute myeloid leukemia or myelodysplasia receiving allogeneic hematopoietic cell transplantation. *J Clin Oncol* 2007;**25**:4246–54.
38. Scott BL, Storer B, Loken MR, Storb R, Appelbaum FR, Deeg HJ. Pretransplantation induction chemotherapy and posttransplantation relapse in patients with advanced myelodysplastic syndrome. *Biol Blood Marrow Transplant* 2005;**11**:65–73.
39. Warlick ED, Cioc A, Defor T, Dolan M, Weisdorf D. Allogeneic stem cell transplantation for adults with myelodysplastic syndromes: importance of pretransplant disease burden. *Biol Blood Marrow Transplant* 2009;**15**:30–8.
40. Nakai K, Kanda Y, Fukuhara S, *et al.* Value of chemotherapy before allogeneic hematopoietic stem cell transplantation from an HLA-identical sibling donor for myelodysplastic syndrome. *Leukemia* 2005;**19**:396–401.

Supporting Information

Additional Supporting Information may be found in the online version of this article:

Figure S1. Semilandmark plots illustrating impact of chronic GVHD on OS of patients with MDS receiving allo-HCT.

Table S1. Univariate analysis for NRM, relapse, and OS.

Table S2. Multivariate analysis for NRM, relapse and OS in the RIC group (patients pretreated with RIC).

Int J Hematol (2013) 97:421–426
DOI 10.1007/s12185-013-1297-9

ORIGINAL ARTICLE

Diagnosis and evaluation of intestinal graft-versus-host disease after allogeneic hematopoietic stem cell transplantation following reduced-intensity and myeloablative conditioning regimens

Satoshi Yamasaki · Akiko Miyagi-Maeshima · Yasuo Kakugawa · Yoshihiro Matsuno · Fusako Ohara-Waki · Shigeo Fuji · Yuriko Morita-Hoshi · Masakazu Mori · Sung-Won Kim · Shin-ichiro Mori · Takahiro Fukuda · Ryuji Tanosaki · Tadakazu Shimoda · Kensei Tobinai · Daizo Saito · Yoichi Takaue · Takanori Teshima · Yuji Heike

Received: 10 August 2012 / Revised: 7 February 2013 / Accepted: 8 February 2013 / Published online: 23 February 2013

Abstract Colonoscopic evaluation of mucosal tissues after allogeneic hematopoietic stem cell transplantation (HSCT) is very useful in evaluating pathogenesis and diagnosis of intestinal graft-versus-host disease (GVHD). However, information on the timing and sites of biopsies and the immunohistological evaluation of mucosal tissues for diagnosing intestinal GVHD, especially following reduced-intensity (RIC) regimens, remains very limited. A total of 33 patients with histologically proven GVHD after allogeneic HSCT with RIC ($n = 23$) and myeloablative conditioning (MAC, $n = 10$) regimens were enrolled in the present study. Colonoscopy was performed due to gastrointestinal symptoms, especially diarrhea and anorexia. Sites of biopsies with the worst histopathological grading were the terminal ileum in 67 % of patients. In the RIC group, the onset of diarrhea prior to colonoscopy examination was later (median: RIC, 57 vs. MAC, 27 days) and the number of patients who developed abdominal pain tended to be higher (RIC, 70 % vs. MAC, 30 %). A lower number of CD4+ cells and a higher ratio of Foxp3+ cells to CD4+ cells were detected in the involved lesions of intestinal GVHD following RIC. These differences in the RIC and MAC groups suggest that regimen-specific therapeutic strategies are required for diagnosing intestinal GVHD.

Keywords Intestinal graft-versus-host disease · Allogeneic hematopoietic stem cell transplantation · Reduced-intensity regimen · HLA-matched donor · Colonoscopy

S. Yamasaki · F. Ohara-Waki · S. Fuji · Y. Morita-Hoshi · M. Mori · S.-W. Kim · S. Mori · T. Fukuda · R. Tanosaki · K. Tobinai · Y. Takaue · Y. Heike (✉)
Division of Hematology/Hematopoietic Stem Cell Transplantation, National Cancer Center Hospital, 5-1-1 Tsukiji, Chuo-ku, Tokyo 104-0045, Japan
e-mail: yheike@ncc.go.jp

S. Yamasaki · T. Teshima
Department of Medicine and Biosystemic Sciences, Faculty of Medicine, Kyushu University, Fukuoka, Japan

A. Miyagi-Maeshima · Y. Matsuno · T. Shimoda
Division of Pathology, National Cancer Center Hospital, Tokyo, Japan

Y. Kakugawa · D. Saito
Endoscopy Division, National Cancer Center Hospital, Tokyo, Japan

T. Teshima
Center for Cellular and Molecular Medicine, Kyushu University Hospital, Fukuoka, Japan

Introduction

Acute graft-versus-host disease (GVHD) develops when donor alloreactive T cells recognized alloantigens expressed on host antigen-presenting cells and attack host target epithelium [1]. Many other immune cells, such as Foxp3+ regulatory T (Treg) cells, NKT cells and NK cells, are involved in the pathogenesis of GVHD [2–6]. In addition, damage to host tissue, particularly the gastrointestinal (GI) tract, mainly caused by the conditioning regimen, results in the translocation of endotoxin across damaged mucosal barriers, which augments the cytokine cascade [7, 8]. According to this notion, the use of reduced-intensity conditioning (RIC) regimens could have a favorable impact on the incidence and characteristics of GVHD. In fact, it has been reported that the incidence of GVHD was lower in patients after RIC than myeloablative conditioning (MAC, [9]).

Precise pathological evaluation of the GI tract may provide valuable information about the occurrence of GVHD. Hence, in the present study, we examined biopsy samples obtained by colonoscopy from patients, who suffered from intestinal GVHD after allogeneic hematopoietic stem cell transplantation (HSCT) with RIC or MAC regimens, to evaluate the characteristics of cells infiltrating into the intestinal mucosa.

Patients and methods

Patient characteristics

This study included 258 adult Japanese patients with hematologic malignancies who had undergone their first allogeneic HSCT from a human leukocyte antigen (HLA) matched related ($n = 168$) or unrelated donor ($n = 90$) between January 2002 and May 2006 at the National Cancer Center Hospital in Japan. Typing for HLA-A, -B, and -DR antigens of the donor and recipient was performed by low-resolution DNA typing. RIC regimens consisted of the combination of busulfan (BU, 8 mg/kg) and fludarabine (Flu, 180 mg/m^2; $n = 95$) or 2-chlorodeoxyadenosine (2-CdA, 0.66 mg/kg; $n = 41$) with antithymocyte globulin (ATG, 5–10 mg/kg; $n = 5$) or 2–4 Gy total body irradiation (TBI, $n = 21$), whereas MAC regimens consisted of cyclophosphamide (CY, 120 mg/kg) in combination with either 12 Gy TBI ($n = 38$) or BU (16 mg/kg, $n = 51$) with cytarabine ($n = 3$). GVHD prophylaxis included cyclosporine (CSP) or tacrolimus (TAC) from day −1, with 159 patients receiving short courses of methotrexate (MTX).

Definition of transplant outcomes

Neutrophil engraftment was defined as an absolute neutrophil count (ANC) exceeding 0.5×10^9/L for 3 consecutive days after transplantation. The day of neutrophil engraftment was determined to be the first of these 3 consecutive days. Regimen-related toxicity (RRT) of organ systems which developed within 100 days was graded according to the criteria proposed by the National Cancer Institute-Common Terminology Criteria for Adverse Events v4.0 (CTCAE v4.0). GI symptoms were graded similarly. The onset of acute GVHD and its severity was graded by consensus criteria [10]. Classic or late-onset acute GVHD was distinguished by the time of onset, i.e., whether it developed within or later than 100 days of transplantation, respectively [11]. Patients with Grades II–IV acute GVHD were treated with prednisolone (PSL) according to a standard regimen [12].

Colonoscopic evaluation

All colonoscopies were performed using an Olympus colonoscope (PCF-Q240ZI; Olympus Optical Co., Ltd, Tokyo, Japan). Biopsies of 65 allografted patients were taken at a first colonoscopy examination after transplantation when neutrophil recovery occurred and GVHD was suspected due to GI symptoms including nausea, vomiting, abdominal pain, anorexia and diarrhea. In all cases, microbiologic standard evaluation of stool including screening for *Clostridium difficile* toxin and surveillance with cytomegalovirus (CMV)-antigenemia tested by direct immunoperoxidase staining of leukocytes with peroxidase-labeled monoclonal antibody was performed. Patients receiving preemptive antiviral drugs for CMV-antigenemia or suffering from CMV-colitis were defined as clinical CMV infection. As controls, we evaluated 36 samples from 18 patients who had colorectal cancer and underwent colorectostomy after endoscopic mucosal resection. We confirmed that all these latter samples were negative for cancer cells.

Histological evaluation and immunohistochemistry

Biopsy samples were stained with hematoxylin and eosin, and graded microscopically based on a scale adapted from histological criteria [13] as follows: Grade I, single cell necrosis and apoptosis noted on medium power; Grade II, evidence of epithelial damage by crypt/glandular abscess, epithelial flattening or crypt/glandular dilation; Grade III, dropout of one or more crypts/glands; and Grade IV, total epithelial denudation.

Immunostaining was performed based on the dextran polymer method by use of the Envision + kit (DakoCytomation). Briefly, serial 4 μm sections were cut, deparaffinized and subjected to a heat-induced epitope retrieval step using the autoclave technique before incubation with antibodies. The sections were rinsed in cool running water, washed in phosphate-buffered saline, and incubated with antibodies. These were mouse monoclonals against CD3 (clone PS1, 1:50 dilution, Novocastra, UK), CD4 (clone 1F6, 1:50, Novocastra), CD8 (clone 4B11, 1:50, Novocastra), CD25 (clone 4C9, 1:1000, Novocastra), CD56 (clone Lu-243, 1:200, Novocastra), TIA-1 (clone 2G9A10F5, 1:1000, Beckman Coulter, USA), Granzyme B (clone GrB-7, 1:200, DakoCytomation), Foxp3 (clone ab22510, 1:50, Abcam, UK), and anti-CMV antigens (clones CCH2 + DDG9, 1:50 dilution, DakoCytomation). Bound antibodies were visualized by the 3,3′-diaminobenzidine tetrahydrochloride reaction. All slides were counterstained lightly with hematoxylin and mounted for microscopic examination, and then coded and read in a blinded fashion. Each observer estimated the number of

positive cells per 10 high-power fields (×400 microscopic fields, 10 HPF), using an Olympus BX40 microscope (Olympus, Tokyo, Japan). Samples of reactive lymphoid hyperplasia in the tonsil served as a positive control. Mouse N-universal negative control (cocktail of mouse IgG1, IgG2a, IgG2b, IgG3 and IgM; DakoCytomation) was run concurrently. In all cases, the clinical records and the results of routine histology performed at diagnosis were reviewed.

A retrospective analysis was performed on paraffin wax-embedded tissue samples from 65 patients, obtained from multiple sites where there appeared to be mucosal abnormalities. This study was approved by the Ethics Committee, and all patients provided informed consent.

Statistical analysis

Comparisons of variables were performed using the two-tailed Fisher exact test or the Chi-square test. Continuous variables were compared by the Mann–Whitney *U* test. Results of cell enumerations were expressed as means ± SEM. All *P* values were two-sided with type I error rate fixed at 0.05.

Results

Clinical features

Thirty-three patients (51 %, 33/65) were diagnosed as histologically proven GVHD by biopsy samples (RIC, 17 %; 23/136 vs. MAC, 11 %; 10/89; $P = 0.081$). Fourteen patients (22 %, 14/65) as histologically proven GVHD with clinical CMV infection, 12 (18 %, 12/65) as clinical CMV infection without GVHD, 5 (8 %, 5/65) as histologically proven GVHD with both clinical CMV and *Clostridium difficile* infections, or 1 (1 %, 1/65) as histologically proven GVHD with *Clostridium difficile* infection were excluded. Patient characteristics and transplant outcomes in 33 patients with histological proven GVHD are summarized in Table 1. There were significant differences between the RIC and MAC groups in the number of related donors (RIC, 83 % vs. MAC, 40 %; $P = 0.035$), the number of patients who were given MTX for GVHD prophylaxis (RIC, 35 % vs. MAC, 100 %; $P = 0.00050$), the time to neutrophil engraftment (median: RIC 12 vs. MAC 15 days) and the incidence of RRT Grade 3 (RIC, 9 % vs. MAC, 50 %). Prednisolone (PSL) for the treatment of acute GVHD was administered after colonoscopy with

Table 1 Patient characteristics and transplant outcomes

	RIC ($n = 23$)	MAC ($n = 10$)	*P*
Median age of patients (range)	53 (27–63)	48 (25–57)	0.12
Median age of donors (range)	48 (22–65)	37 (29–54)	0.072
Male/female patient	19/4	7/3	0.65
Female donor for male patient	6	2	0.99
Diagnosis			
Acute myeloid leukemia	3	4	0.28
Acute lymphoblastic leukemia	1	2	
Chronic myeloid leukemia	3	0	
Malignant lymphoma	11	2	
Myelodysplastic syndrome	4	2	
Myelofibrosis	1	0	
Donor type (related/unrelated)	19/4	4/6	0.035
Stem cell source (BM/PBSC)	7/16	6/4	0.14
GVHD prophylaxis (CSP or TAC alone/MTX with CSP or TAC)	15/8	0/10	0.00050
Median day to neutrophil engraftment (range)	12 (9–20)	15 (10–31)	0.036
RRT (Grade 3/4)	2/0	5/0	0.016
Acute GVHD (Grade II/III/IV)	4/13/1	6/4/0	0.12
Median onset day (range) of Grade II–IV acute GVHD	28 (14–99)	22 (11–66)	0.10
Use of PSL for GVHD therapy			
0.5 to <1.0/1.0 to <2.0/≥2.0 mg of PSL/kg	2/10/6	3/1/3	0.20
Stage of GI tract 1/2/3/4	3/4/9/1	4/2/2/0	0.45

RIC reduced-intensity regimen, *MAC* myeloablative regimen, *BM* bone marrow, *PBSC* peripheral blood stem cell, *CSP* cyclosporine, *TAC* tacrolimus, *MTX* methotrexate, *RRT* regimen-related toxicity, *GVHD* graft-versus-host disease, *PSL* prednisolone, *GI* gastrointestinal

Table 2 Presenting gastrointestinal symptoms, laboratory data, and clinical and histological diagnosis at the time of biopsy

	RIC	MAC	*P*
Median day of biopsy (range)	63 (14–158)	32 (11–120)	0.11
Gastrointestinal symptoms			
Diarrhea (Grade 1/2/3)	2/4/17	2/3/5	0.40
Median (range) onset day	57 (10–145)	27 (9–103)	0.050
Median (range) duration day[a]	5 (1–16)	5 (2–23)	0.40
Stools/day, median (range)	7 (2–16)	6 (1–14)	0.15
Nausea (Grade 1/2/3)	2/2/7	2/4/2	0.090
Vomiting (Grade 1/2/3)	5/3/0	5/2/0	0.16
Abdominal pain (Grade 1/2/3)	2/6/8	2/1/0	0.054
Anorexia (Grade 1/2/3)	1/0/22	0/2/8	0.073
Laboratory data, median (range)			
WBC ($\times 10^9$/L)	5.2 (1.0–24.2)	4.1 (2.5–23.8)	0.36
Hemoglobin (g/dL)	10.3 (5.6–14.2)	8.2 (7.1–13.0)	0.14
Albumin (g/dL)	3.0 (1.8–4.2)	3.1 (1.7–3.8)	0.98
Total serum bilirubin (mg/dL)	0.7 (0.3–11.8)	0.8 (0.3–3.1)	0.98
Acute GVHD at the biopsy (Grade II/III/IV)	5/15/1	4/4/0	0.42
Classic/late-onset	16/7	8/2	0.69
Stage of GI tract 1/2/3/4	5/6/8/1	4/2/2/0	0.71
Median onset day (range) of acute GVHD with the GI tract	27 (10–99)	22 (11–66)	0.31
Worst histological grading (Grade I/II/III/IV)	9/0/4/10	3/0/5/2	0.14
Sites of biopsies (Terminal ileum/Colon/Rectum)	15/6/2	7/3/0	0.63

[a] Time from onset of diarrhea to colonoscopy examination

biopsies. In patients with histologically proven GVHD, presenting GI symptoms, laboratory data at the time of biopsy, and clinical and histological GVHD diagnosis are summarized in Table 2. In these patients, colonoscopy was performed for GI symptoms including diarrhea ($n = 33$), nausea ($n = 19$), vomiting ($n = 15$), abdominal pain ($n = 19$) and anorexia ($n = 33$). The onset of diarrhea was significantly later in the RIC than the MAC group (median: RIC, 57 vs. MAC, 27 days; range, 10–145 vs. 9–103, respectively; $P = 0.050$). The number of patients who developed abdominal pain tended to be higher in the RIC than the MAC group (RIC, 70 % vs. MAC, 30 %; $P = 0.054$).

Infiltrating cell type in the intestinal mucosa

All 167 samples were classified as histologically proven GVHD and each of the biopsy samples diagnosed as having the worst histopathological grading [13] was selected for the evaluation of infiltrating cells. In 67 % of patients, the sites of biopsies with the worst histopathological grading were the terminal ileum.

Using standard immunohistological techniques, the number and phenotype of mucosa-infiltrating cells was determined in intestinal biopsy samples from the 33 allografted patients with histologically proven GVHD. The number of CD4+ cells was significantly lower in the RIC than the MAC group (RIC, 333 ± 122 vs. MAC, 522 ± 142 per 10 HPF, respectively; $P = 0.042$: Table 3 and Fig. 1a). The ratio of Foxp3+ cells to CD4+ cells was higher in the RIC than the MAC group (RIC, 61 ± 16 vs. 7 ± 2 per 10 HPS, respectively; $P = 0.034$: Fig. 1b).

Table 3 Phenotype of infiltrating cells in intestinal biopsy samples measured by immunoenzymatic labeling

	RIC	MAC	*P*	Control
Cell type				
CD3+	922 ± 158[a]	1126 ± 230	0.35	661 ± 53
CD4+	333 ± 122	522 ± 142	0.042	334 ± 44
CD8+	583 ± 65	609 ± 139	0.84	293 ± 33
CD25+	77 ± 21	76 ± 22	0.83	51 ± 11
CD56+	29 ± 7	23 ± 8	0.60	32 ± 4
TIA-1+	443 ± 68	323 ± 71	0.33	181 ± 38
Granzyme B+	10 ± 2	5 ± 2	0.38	4 ± 1
Foxp3+	79 ± 22	63 ± 26	0.54	49 ± 11
Foxp3+/CD4+ ($\times 10^{-2}$)	61 ± 16	7 ± 2	0.034	7 ± 1
Foxp3+/CD8+ ($\times 10^{-2}$)	14 ± 3	19 ± 9	0.99	18 ± 4

[a] Mean ± SEM

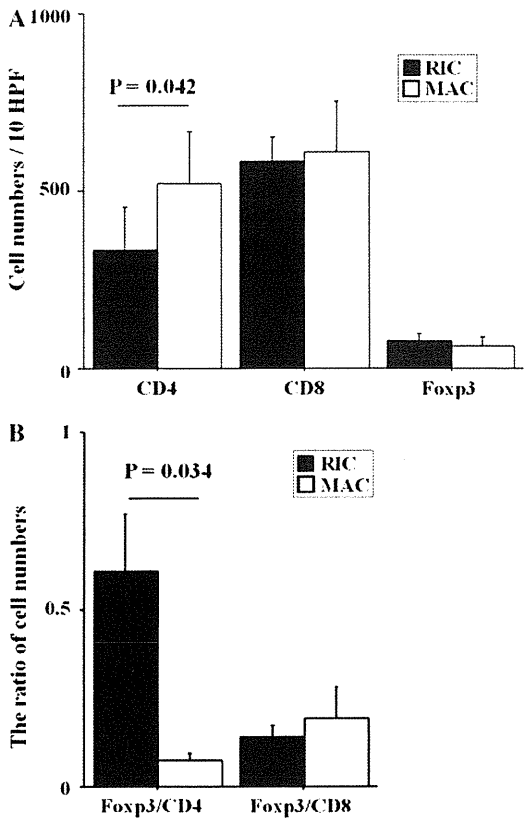

Fig. 1 Comparison of the cell numbers per 10 HPF in intestinal control and biopsy samples. Paraffin-embedded intestinal biopsy samples with signs of GVHD following RIC (n = 23) and MAC (n = 10) regimens were stained for CD4, CD8, and Foxp3 by immunohistochemistry. The numbers of CD4+, CD8+, and Foxp3 cells (**a**) or the ratios of Foxp3+ cells to CD4+ and CD8+ cells (**b**) were counted per 10 high-power fields (×400, 10 HPF). The results show the mean ± SEM

Discussion

Precise information on the timing and sites of biopsies and the immunohistological evaluation of mucosal tissues after intestinal GVHD, especially in the RIC group, which is very useful in evaluating pathogenesis and diagnosis of GVHD, has been very limited. The results of the present study provide some evidence supporting the notion that there are some differences in intestinal GVHD between the RIC and MAC groups, such as the onset of diarrhea prior to colonoscopy examination was significantly later in the RIC group and the number of patients who developed abdominal pain tended to be higher in the RIC group. The number of CD4+ cells was decreased and the ratio of Foxp3+ cell to CD4+ cells was increased in the RIC group.

In the patients who received colonoscopy, all these patients took an examination when neutrophil recovery occurred and GVHD was suspected due to GI symptoms, especially diarrhea and anorexia. Further studies are needed to detect the marker including the suitable timing of biopsies, i.e., GI symptoms, such as the onset of diarrhea and abdominal pain, for diagnosing an early stage of intestinal GVHD following RIC regimens in all patients who received allogeneic HSCT with and without intestinal GVHD, but prolonged or intensified periods for GVHD prophylaxis may be important to prevent the later onset of intestinal GVHD in the RIC group.

In this study, the sites of biopsies selected for the evaluation of infiltrating cells were those with the worst histopathological grading. This was the terminal ileum in 67 % of patients regardless of RIC and MAC groups. In addition, all samples were classified as histologically proven GVHD. These results suggest that GVHD following both RIC and MAC regimens is possible to be diagnosed at any sites of colon, while samples obtained from the terminal ileum by colonoscopy are more useful for finding severe GVHD lesions than those obtained from other sites, in agreement with previous reports [14].

There were significant differences in the characteristics of infiltrating CD4+ cells between the RIC and MAC groups probably due to the use of adenine nucleoside analog, i.e., fludarabine or chlorodeoxyadenosine, which has a suppressive effect on T cells, predominantly CD4+ cells [15]. Our data could not show the data that agree with murine studies that RIC regimens are associated with less tissue damage and cytokine secretion [16]. However, we should recognize the possibility of overestimating the incidences of intestinal GVHD in the RIC group because there was no difference in the incidence of intestinal GVHD between the RIC and MAC groups probably due to the differences in the patient characteristics, such as the number of related donors and the number of patients given MTX for GVHD prophylaxis, which may influence the repairing process in the intestinal mucosa. The Foxp3+/CD4+ ratio in infiltrating lymphocytes was higher in the RIC than MAC group, indicating that we should not reduce the intensity of GVHD prophylaxis and omit MTX for GVHD in the RIC groups. Because intestinal CD4+ cells and Foxp3+ Tregs play an important role in immunological homeostasis preventing uncontrolled inflammation against intestinal bacteria, whereas the effector phase with damage in the RIC regimen may be different from that in the MAC regimen. Although Foxp3+ Tregs are important for preventing intestinal GVHD [6, 17], the number of infiltrating Foxp3+ Tregs may not be enough to prevent intestinal GVHD, but the balance of infiltrating CD4+ cells and Foxp3+ Tregs might be important. To compare the characteristics of cells infiltrating into the intestinal mucosa, studying the pathophysiological feature of infiltrating lymphocytes may be a useful, but not appear to support these previous data, because of the limitation of colonoscopy examination, such as timing and sites of biopsies.

In summury, our results suggest that GI symptoms, not only diarrhea but abdominal pain, are possible to have been useful for diagnosing intestinal GVHD using colonoscopy, especially in the RIC group. Compared with the MAC group, later onset, lower CD4+ cells, and higher Foxp+/CD4+ ratio in the RIC group indicate that we need to adjust the therapeutic procedures of intestinal GVHD after RIC regimen, including prolonged or intensified periods for GVHD prophylaxis and treatment, using conventional MTX and PSL as well as additional secondary therapies at the beginning, i.e., MMF or ATG.

Acknowledgments We appreciate the work of the staff of hematopoietic stem cell transplantation unit, National Cancer Center Hospital in Japan, who provided excellent patient and donor care. We would like to express thanks to Ms. Miura and Kina for their kind technical assistance.

References

1. Shlomchik WD, Couzens MS, Tang CB, McNiff J, Robert ME, Liu J, et al. Prevention of graft versus host disease by inactivation of host antigen-presenting cells. Science. 1999;285:412–5.
2. Zeng D, Lewis D, Dejbakhsh-Jones S, Lan F, Garcia-Ojeda M, Sibley R, et al. Bone marrow NK1.1(-) and NK1.1(+) T cells reciprocally regulate acute graft versus host disease. J Exp Med. 1999;189:1073–81.
3. Ruggeri L, Capanni M, Urbani E, Perruccio K, Shlomchik WD, Tosti A, et al. Effectiveness of donor natural killer cell alloreactivity in mismatched hematopoietic transplants. Science. 2002;295:2097–100.
4. Edinger M, Hoffmann P, Ermann J, Drago K, Fathman CG, Strober S, et al. CD4+ CD25+ regulatory T cells preserve graft-versus-tumor activity while inhibiting graft-versus-host disease after bone marrow transplantation. Nat Med. 2003;9:1144–50.
5. Passweg JR, Stern M, Koehl U, Uharek L, Tichelli A. Use of natural killer cells in hematopoietic stem cell transplantation. Bone Marrow Transpl. 2005;35:637–43.
6. Rezvani K, Mielke S, Ahmadzadeh M, Kilical Y, Savani BN, Zeilah J, et al. High donor FOXP3-positive regulatory T-cell (Treg) content is associated with a low risk of GVHD following HLA-matched allogeneic SCT. Blood. 2006;108:1291–7.
7. Hill GR, Crawford JM, Cooke KR, Brinson YS, Pan L, Ferrara JL. Total body irradiation and acute graft-versus-host disease: the role of gastrointestinal damage and inflammatory cytokines. Blood. 1997;90:3204–13.
8. Reddy P, Ferrara JL. Immunobiology of acute graft-versus-host disease. Blood Rev. 2003;17:187–94.
9. Perez-Simon JA, Diez-Campelo M, Martino R, Brunet S, Urbano A, Caballero MD, et al. Influence of the intensity of the conditioning regimen on the characteristics of acute and chronic graft-versus-host disease after allogeneic transplantation. Br J Haematol. 2005;130:394–403.
10. Przepiorka D, Weisdorf D, Martin P, Klingemann HG, Beatty P, Hows J, et al. 1994 consensus conference on acute GVHD grading. Bone Marrow Transpl. 1995;15:825–8.
11. Pavletic SZ, Lee SJ, Socie G, Vogelsang G. Chronic graft-versus-host disease: implications of the National Institutes of Health consensus development project on criteria for clinical trials. Bone Marrow Transpl. 2006;38:645–51.
12. Doney KC, Weiden PL, Storb R, Thomas ED. Treatment of graft-versus-host disease in human allogeneic marrow graft recipients: a randomized trial comparing antithymocyte globulin and corticosteroids. Am J Hematol. 1981;11:1–9.
13. Sale GE, Shulman HM, McDonald GB, Thomas ED. Gastrointestinal graft-versus-host disease in man. A clinicopathologic study of the rectal biopsy. Am J Surg Path. 1979;3:291–9.
14. Thompson B, Salzman D, Steinhauer J, Lazenby AJ, Wilcox CM. Prospective endoscopic evaluation for gastrointestinal graft-versus-host disease: determination of the best diagnostic approach. Bone Marrow Transpl. 2006;38:371–6.
15. Bergmann L, Fenchel B, Jahn B, Mitrous PS, Hoelzer D. Immunosuppressive effects and clinical response of fludarabine in refractory chronic lymphocytic leukemia. Ann Oncol. 1993;4:371–5.
16. Ferrara JL, Reddy P. Pathophysiology of graft-versus-host disease. Semin Hematol. 2006;43:3–10.
17. Rieger K, Loddenkemper C, Maul J, Fietz T, Wolff D, Terpe H, et al. Mucosal FOXP3+ regulatory T cells are numerically deficient in acute and chronic GvHD. Blood. 2006;107:1717–23.

Bone Marrow Transplantation (2010) 45, 1594–1601

www.nature.com/bmt

ORIGINAL ARTICLE

Identification of molecular markers for pre-engraftment immune reactions after cord blood transplantation by SELDI-TOF MS

Y Morita-Hoshi[1], S-I Mori[1], A Soeda[1], T Wakeda[1], Y Ohsaki[2], M Shiwa[2], K Masuoka[3], A Wake[3], S Taniguchi[3], Y Takaue[1] and Y Heike[1]

[1]*Department of Medical Oncology, National Cancer Center Hospital, Tokyo, Japan;* [2]*Bio-Rad Laboratories, K.K., Kanagawa, Japan and* [3]*Department of Hematology, Toranomon Hospital, Tokyo, Japan*

Cord blood transplantation (CBT) is frequently associated with pre-engraftment immune reaction (PIR), which is characterized by high-grade fever that peaks around day 9 of transplantation. PIR mimics hyperacute GVHD or engraftment syndrome; however, it is considered to be of different etiology as it occurs before engraftment. Proteomic patterns have been studied in the fields of transplantation, but no specific marker has been identified. As there are no data to confirm the mechanism of PIR, we used a surface-enhanced laser desorption/ionization time-of-flight mass spectroscopy (SELDI-TOF MS) system to identify a specific marker for PIR. The protein expression profile of serum samples from CBT patients was analyzed with a SELDI-TOF MS system. A protein peak that commonly predominated in PIR was purified by an anion exchange column, isolated by SDS-PAGE, and identified by in-gel trypsin digestion, and mass fingerprinting. A 8.6-kDa protein and 11-kDa protein that increased by 10- to 100-fold in the serum of patients during PIR was identified as anaphylatoxin C4a and serum amyloid A. SELDI-TOF MS system in combination with other proteomic methods could serve as a potential diagnostic tool in discovering biomarkers for PIR after CBT.
Bone Marrow Transplantation (2010) **45,** 1594–1601; doi:10.1038/bmt.2010.18; published online 15 March 2010
Keywords: serum amyloid A; pre-engraftment immune reactions; cord blood transplantation; SELDI-TOF MS

Introduction

High-grade fever before engraftment without any other obvious signs of infection, which mimics hyperacute GVHD or engraftment syndrome, is frequently observed in patients who undergo cord blood transplantation (CBT).[1,2] In previous reports, when patients with no evidence of infection or adverse effects of medication exhibited skin eruption, diarrhea, jaundice or body weight gain greater than 10% of baseline, these conditions were defined as 'immune reactions.' These reactions were classified as 'pre-engraftment immune reaction (PIR)' if they developed 6 or more days before engraftment, whereas those within 5 days of engraftment were defined as 'engraftment syndrome' (1). The reported incidence of PIR has ranged from 78–83% (1–2). This PIR peaks at around day 9 of CBT, and is often accompanied by high-grade fever. Although PIR responds well to corticosteroid therapy, the prolonged use of steroid often causes an increased incidence of infectious complications, leading to significant treatment-related mortality, particularly in the elderly. GVHD prophylaxis with tacrolimus, compared with CsA, is less likely to be associated with PIR[3,4] and the addition of MTX may further reduce the risk.[5,6] It has been speculated that cytokines induced by the initial immune/inflammation reaction are the primary cause of PIR, but no data are available to confirm this supposition. To clarify this question, we evaluated the protein expression profile of serum in CBT recipients using a surface-enhanced laser desorption/ionization time-of-flight mass spectroscopy (SELDI-TOF MS) system and found potential markers for PIR.

Materials and methods

Study patients and samples

Patients who received treatment for hematological malignancies at the National Cancer Center Hospital or Toranomon Hospital between February 2002 and May 2005 were included in this study. The study was approved by the Ethics Committee, and written informed consent was given by all patients. A total of 78 peripheral blood samples taken from 57 patients, including 34 samples taken from 13 patients who had undergone allogeneic CBT, were eligible for the analysis. Samples from CBT patients were taken on three different occasions, that is, (1) afebrile period before PIR onset: the median of day 3 (1–6) post transplant; (2) onset of fever: the median of day 8 (6–13); and (3) after resolution of fever: the median of day 26.5 (15–60). To analyze the protein profile that was specific to PIR, samples taken from patients with documented infection

Correspondence: Dr Y Heike, Department of Medical Oncology, National Cancer Center Hospital, 5-1-1 Tsukiji Chuo-ku, Tokyo 104-0045, Japan.
E-mail: yheike@ncc.go.jp
Received 14 July 2009; revised 24 December 2009; accepted 27 December 2009; published online 15 March 2010

Table 1 Characteristics of 13 patients

Age	
Median 52 years	
Range (26–70 years)	
Sex	
Male	6
Female	7
Primary disease	
AML	5
ALL	2
Adult T-cell leukemia	2
Diffuse large B-cell lymphoma	2
Peripheral T-cell lymphoma-unspecified	1
Myelofibrosis	1
Conditioning regimen	
Flu 180 mg/m^2, BU 8 mg/kg, TBI 4 Gy	6
Flu 180 mg/m^2, BU 8 mg/kg, TBI 8 Gy	1
Flu 125 mg/m^2, Mel 80 mg/m^2, TBI 4 Gy	5
Flu 125 mg/m^2, Mel 80 mg/m^2, TBI 2 Gy	1
GVHD Prophylaxis	
CsA	6
CsA + short-term MTX	4
Tacrolimus	3
No. of HLA mismatch	
1 locus	3
2 loci	9
4 loci	1
Day of engraftment (n = 11)	
Median 18 days	
Range 13–29 days	
Day of PIR onset	
Median 8 days	
Range 6–13 days	
Day between PIR and resolution	
Median 15.5 days	
Range 7–49 days	
Treatment for PIR	
None	3
Empiric antibiotics	4
Corticosteroids and empiric antibiotics	6

Abbreviations: Flu = fludarabine; Mel = melphalan; PIR = pre-engraftment immune reaction.

or those who were suffering from engraftment syndrome were excluded from the analysis. All 13 CBT patients received reduced-intensity conditioning, and graft rejection occurred in 2 patients (16%). As for the treatment and its outcome for PIR, six patients responded well to corticosteroid and seven patients improved without any treatment or empiric antibiotics alone. One of the patients who developed graft failure received corticosteroids for the treatment of PIR. The mean neutrophil count at PIR was 15 (0–100)/μl. The patients' characteristics are shown in Table 1.

SELDI-TOF MS analysis

The relative protein expression levels were determined as previously described with the following modifications using a SELDI TOF-MS system (Bio-Rad Laboratories, Hercules, CA, USA).[7,8] The protein was processed using a Biomek 2000 Laboratory Work Station (Beckman Coulter, Fullerton, CA, USA). Samples were analyzed in duplicate and 28 spectra were obtained from five serum fractions with four kinds of chips (IMAC30, CM10, H50, Q10), four different binding buffers, two kinds of energy absorption molecules and two focus mass ranges.

Serum fractionation

The serum samples were centrifuged at 20 000 × *g* and the supernatant was vigorously mixed with denaturation buffer U9 (9 M urea: 2% CHAPS: 50 mM Tris-HCl, pH9) for 20 min. Serum samples were fractionated into four fractions by the following methods. Briefly, the strong anion exchange resin BioSepra Q Ceramic HyperD F (Pall, NY, USA) was equilibrated with 50 mM Tris-HCl, pH 9, in advance, and 180 μl per well was loaded onto a filter plate. The loaded resin was equilibrated three times with 200 μl of U1 buffer (U9 buffer diluted 1:10 with 50 mM Tris-HCl). Denatured serum was added to the resin, the sample well was washed with 50 μl of U1 buffer, and the sample was incubated for 30 min at 4 °C. The non-binding fraction was collected, and protein was eluted by a phased pH gradient at pH 5.8, pH 4 and below pH 4.

Protein binding

IMAC30 (immobilized metal affinity capture), CM10 (cation exchange), H50 (reverse-phase) and Q10 (anion exchange) ProteinChip arrays were used for the analysis. To immobilize copper ion on the IMAC30 surface, each spot was incubated with 50 μl of 100 mM copper sulfate for 10 min at room temperature. Excess copper was removed by washing twice with distilled water and incubated with 50 μl of 100 mM sodium acetate (pH 4) for 5 min at room temperature. Each spot was rinsed twice with distilled water before the analysis step.

The following buffers were used for binding and dilution of the samples: 100 mM sodium acetate (pH 4) or 50 mM HEPES (pH 7) for CM10, 100 mM sodium phosphate (pH 7) + 0.5 M NaCl for IMAC30, 50 mM HEPES (pH 7) for H50, and 50 mM Tris-HCl (pH 8) for Q10. The following procedure was commonly used for all chip analyses: (1) Each spot was equilibrated twice with 150 μl of binding buffer on a shaker for 5 min, and excess buffer was removed. (2) The fractionated and unfractionated samples were diluted 10-fold with binding buffer. The diluted samples were loaded onto a chip, and incubated on a shaker for 30 min at room temperature. (3) The chip was washed three times on a shaker for 5 min with 150 μl per spot of buffer. (4) The chip was rinsed twice with 200 μl of distilled water and dried. (5) Each spot was treated with two kinds of energy absorption molecules: 50% saturated sinapinic acid and α-cyano-4-hydroxycinnamic acid.

Protein detection

Captured proteins were detected using a ProteinChip SELDI system (PCS4000 Enterprise, Bio-Rad Laboratories). The maximum detection range was 100 000 with a focus mass range of 3000–10 000 for low MW, and 200 000 with a focus mass range of 10 000–30 000 for high MW. Quantitative analysis of proteins was performed using

ProteinChip Software version 3.2 and ProteinChip Data Manager Software (Bio-Rad Laboratories).

Protein purification and identification

The serum samples were denatured with urea and fractionated by an anion exchange column (ProteinChip Q Spin Columns, Bio-Rad Laboratories) to remove albumin by binding it to the column. The fraction that passed through the anion exchange column at pH 9 was collected. The sample was diluted threefold with 50 mM Tris-HCl (pH 8) and loaded onto an anion exchange column to bind the objective peak protein. The protein was eluted in a phased manner with 50–300 mM NaCl. After demineralization and concentration, the proteins were separated by SDS-PAGE and stained with Coomassie Brilliant Blue. In-gel digestion by Trypsin was performed on the objective band. The protein was determined by mass fingerprinting of the digested peaks against the ProFound database (Rockefeller University

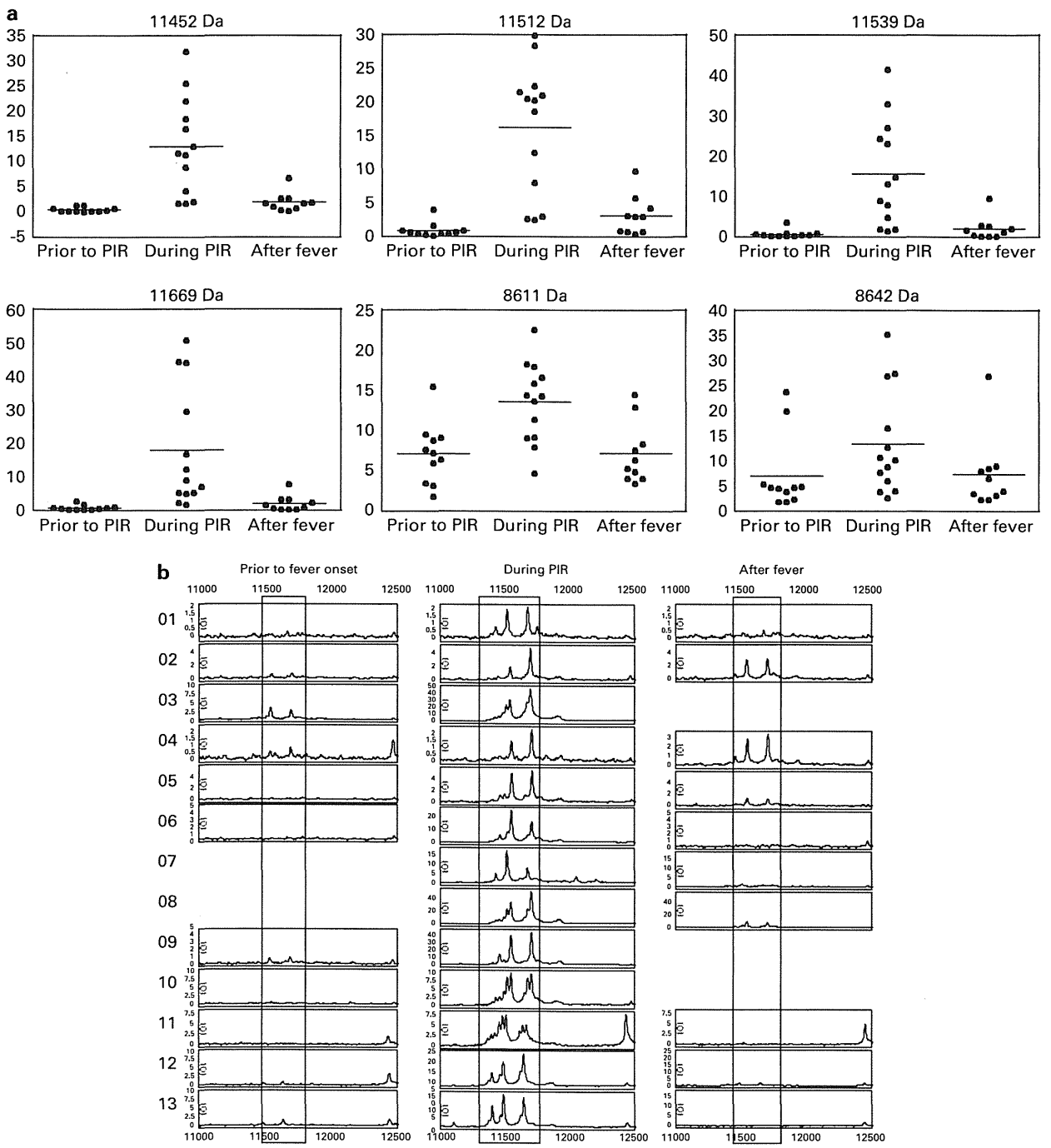

Figure 1 (**a**) Peak intensity levels of six protein peaks that commonly increased at the time of PIR. (**b**) Typical response pattern of the 11-kDa protein peak in 13 patients, in a trace view.

edition), and the amino-acid sequence was determined using the PCI-QSTAR MS/MS search engine.

Statistical analysis

Data were analyzed using ProteinChip Data Manager Software. After baseline correction, MW calibration was performed using eight standard protein molecules followed by a total ion current normalization process. To identify distinct and significant peaks, we used a signal-to-noise cutoff of 2 ($s/n > 2$), which selects peaks with a signal level that is significantly above the calculated background noise.

For the statistical analysis, the Kruskal–Wallis H-test was used to compare differences among three groups. The differences between the two groups were compared with the Wilcoxon–Mann–Whitney *U*-test. Probabilities of $P < 0.05$ were defined as statistically significant.

Results

Protein profiles

A total of 3005 protein peaks for which $s/n > 2$ were detected. Of these, 743 showed a significant difference between the febrile and afebrile periods. After we further excluded noise peaks, 469 peaks still showed a significant difference, and after excluding variations between individuals, 19 candidate peaks that were commonly elevated at PIR in more than 11 patients (84.6%) were selected. Reproducibility was tested, and six protein peaks that commonly increased at the time of PIR, with molecular masses of 8611, 8642, 11452, 11512, 11539 and 11669 Da, were identified (Figure 1). The assay conditions under which the proteins were identified are shown in Table 2.

Purification and determination of target proteins

Protein peaks were fractionated by an anion exchange column, and the elution fraction at pH 9 was used for purification and identification because the albumin that overlaps the candidate peak was removed from this fraction. The protein was eluted from the column with 100–150 mM NaCl. SDS-PAGE after demineralization and concentration of the protein showed an 11-kDa band (Figure 2a). In-gel digestion was performed on the cutout band, and mass fingerprinting was performed for eight peptides with mass values of 1455, 1463, 1550, 1611, 1670, 1706, 1941 and 2097 (Figure 2b). Six of these values were consistent with serum amyloid A (SAA), which consists of

Table 2 Assay conditions by which marker proteins were detected

MW	*Fraction*	*Chip*	*Binding buffer*	*EAM*	*Focus mass range*
8611	pH 9	CM10	100 mM Na Acetate (pH 4)	SPA	3000–10 000
8642	pH 9	CM10	50 mM HEPES (pH 7)	SPA	3000–10 000
11452	Unfractionated	IMAC30	100 mM Na Phosphate (pH 7) + 0.5 M NaCl	SPA	10 000–30 000
11512	Unfractionated	IMAC30	100 mM Na Phosphate (pH 7) + 0.5 M NaCl	SPA	10 000–30 000
	pH 9	CM10	50 mM HEPES (pH 7)	SPA	10 000–30 000
11539	Unfractionated	Q10	50 mM Tris-HCl (pH 8)	SPA	10 000–30 000
11669	Unfractionated	IMAC30	100 mM Na Phosphate (pH 7) + 0.5 M NaCl	SPA	10 000–30 000
	pH 9	CM10	50 mM HEPES (pH 7)	SPA	10 000–30 000
	Unfractionated	Q10	50 mM Tris-HCl (pH 8)	SPA	10 000–30 000

Abbreviations: CM10 = cation exchange; EAM = energy absorption molecule; IMAC30 = immobilized metal affinity capture; SPA = 50% saturated sinapinic acid; Q10 = anion exchange.

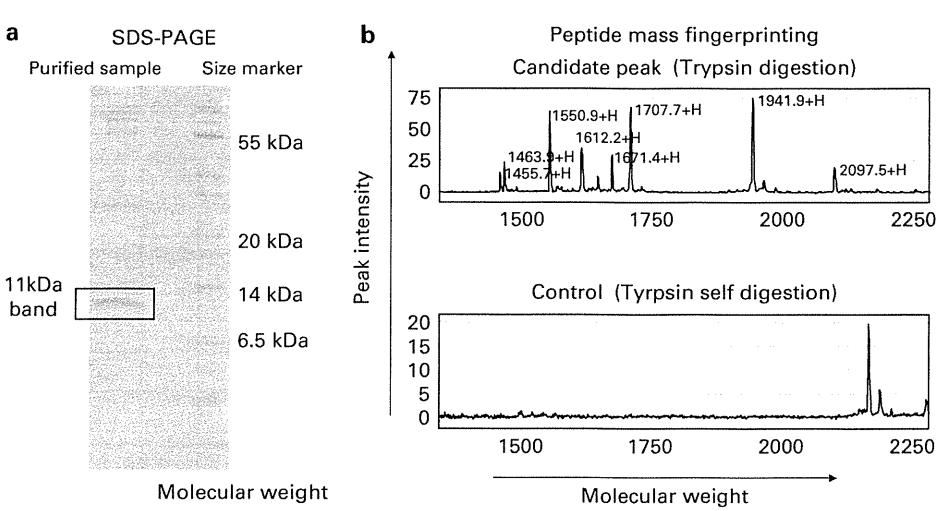

Figure 2 Representative data of SDS-PAGE and peptide mass fingerprinting from the sample taken during PIR. (**a**) SDS-PAGE showing the 11-kDa band. Coomassie Brilliant Blue (CBB) staining. (**b**) Peptide mass fingerprinting of the marker protein.

104 amino acids and has a MW of 11 622, or its isoforms, in which serine and/or arginine is deleted from the N-terminal portion (Figure 3). The amino-acid sequences of all six peptide masses were consistent with SAA by MS/MS analysis.

The SAA level was measured by ELISA in the same sample that was assessed by SELDI-TOF MS. The mean SAA level measured by ELISA before fever onset was 14 (3–51) μg/ml, and this increased to 883 (40–2470) μg/ml at the time of PIR and decreased to 45 (8–126) μg/ml after resolution of the fever (Figure 4a). The data obtained by ELISA agreed with the SELDI-TOF MS peak intensity value (Figure 4b). Although the 8.6 kDa peak was not determined in this experiment, it was most likely to be anaphylatoxin C4a based on its MW (8650) and isoelectric point (9.45).

Serum amyloid A value in different conditions

Seven of the 13 patients with PIR developed acute GVHD, and 2 patients had graft failure. The patients who developed graft failure showed high levels of SAA at PIR (2040 and 2390 μg/ml). The mean and median values of SAA at PIR in seven patients who developed acute GVHD were 677 μg/ml and 451 (60–2470) μg/ml, respectively, which were not significantly different from the values in the four patients without acute GVHD (432 and 506 (40–675) μg/ml) ($P = 0.93$).

The SAA value was assessed in 24 non-transplant febrile patients: (a) 12 samples from patients with documented infection, including sepsis, (b) 6 samples from patients with tumor fever and (c) 6 samples from patients with drug-induced fever. The mean and median values and statistical significance when compared with PIR were (a) 477 μg/ml and 347 (31–1240) μg/ml ($P = 0.63$), (b) 432 μg/ml and 248 (127–1080) μg/ml ($P = 0.75$) and (c) 49 μg/ml and 42 (31–73) μg/ml ($P = 0.0013$), respectively.

The SAA values during acute GVHD in other transplantation settings were assessed in 20 patients: (d) 10 samples from related allo-PBSCT recipients including 5 febrile patients and (e) 10 samples from unrelated BMT recipients including 4 febrile patients. The mean and median values and statistical significance when compared with PIR were (d) 293 and 238 (19–645) μg/ml ($P = 0.20$) and (e) 366 and 344 (31–724) μg/ml ($P = 0.31$), respectively (Figure 4a). The level of SAA elevation was not as high as that in PIR, but the sample size was too small to show specificity.

Discussion

Proteomic analysis has been widely used to assess the allogeneic response, including GVHD in hematopoietic SCT.[8–11] The two most important methods that are used to investigate biomarkers, for example, detection of early GVHD, are SELDI-TOF MS and capillary zone electrophoresis mass spectrometry (CE-MS). Although the resolution and sensitivity of SELDI-TOF MS are not as high as those of CE-MS, it has the benefits of relatively low cost and ease of use.[9] It has been reported that proteomic pattern analysis by SELDI-TOF MS can be used to accurately distinguish GVHD samples from post transplant non-GVHD samples and pretransplant samples with 100% specificity and 100% sensitivity.[8] Furthermore, with the CE-MS system, 16 polypeptide patterns excreted in the urine could be used to discriminate patients with GVHD from patients without complications, with 82% specificity and 100% sensitivity. In addition, 13 sepsis-specific polypeptides

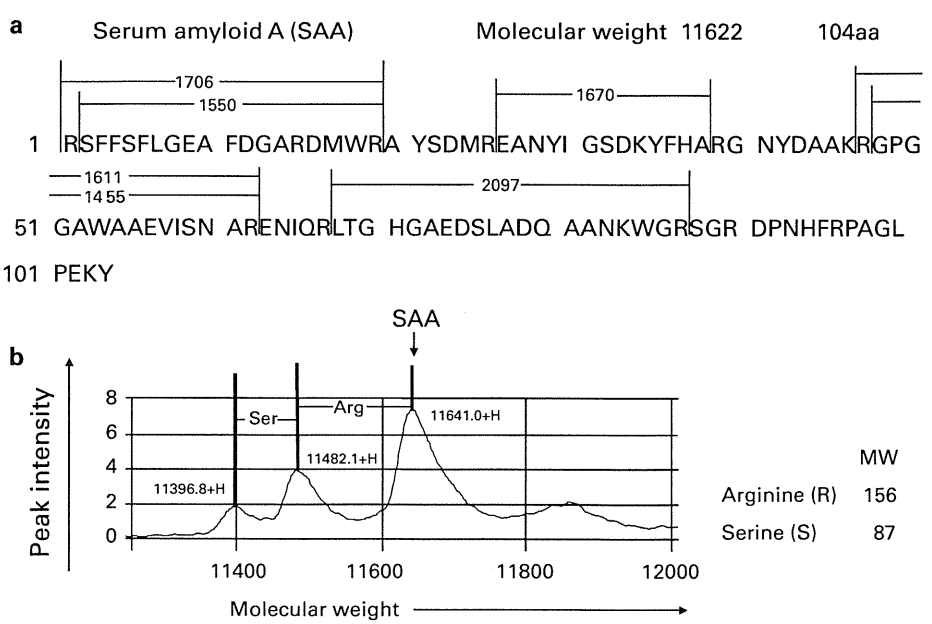

Figure 3 (**a**) Amino-acid sequences of the target protein. Six peptide sequences that matched an MS/MS database search were identical to amino acids of SAA. (**b**) The analyzed peak was determined to be SAA and its isoform produced by the deletion of serine and/or arginine from the N terminus.

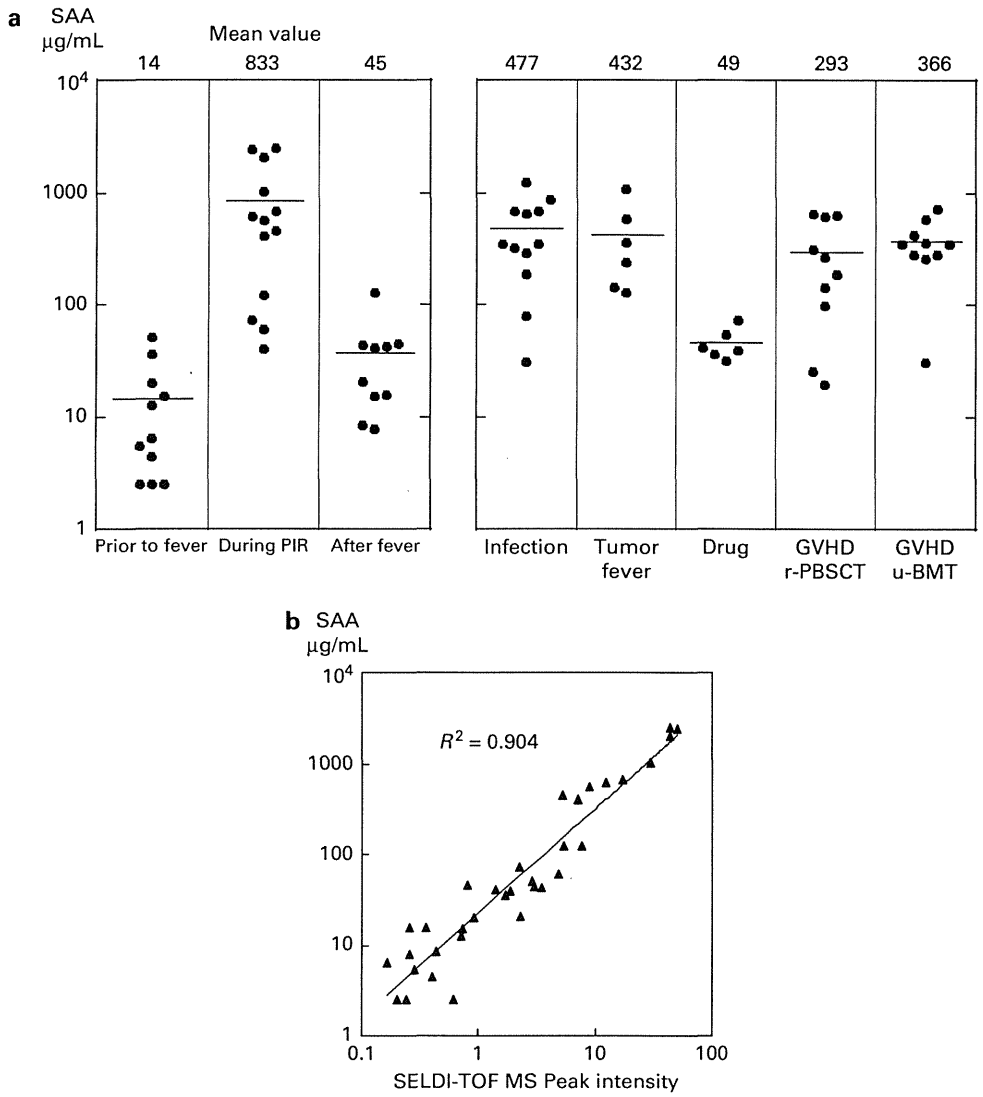

Figure 4 SAA level measured by ELISA. (**a**) SAA level in different conditions: Before fever, during PIR and after fever resolution in 13 CBT recipients. Documented infection including sepsis, tumor fever, drug-induced fever, GVHD in related allo-PBSCT (r-PBSCT) and GVHD in unrelated BMT (u-BMT). (**b**) The data obtained by ELISA correlated well with the SELDI-TOF MS peak intensity value ($n = 34$).

could be used to distinguish sepsis from GVHD, with a specificity of 97% and a sensitivity of 100%.[10] The diagnosis of acute GVHD, even before a clinical diagnosis, is possible with the use of a GVHD-specific model consisting of 31 polypeptides.[11]

Proteomic analysis has also been applied to the analysis of an allograft response in organ transplantation in animal models.[12,13] In a mouse skin transplant model, several protein biomarker candidates were detected by ProteinChip technology based on their molecular mass, which could be used to clearly differentiate between rejection and non-rejection groups, before a clinical manifestation.[12] In a rat small bowel transplantation model, two migration inhibitory factor-related proteins and lysozyme that increased during allograft rejection were identified by a SELDI-TOF MS system.[13] Thus, we believe that ProteinChip technology should be a useful tool for identifying specific markers related to PIR.

Previous studies have shown that combinations of several biomarkers are more sensitive and accurate than the use of a single marker in the diagnosis of an allogeneic response.[11] However, most biomarkers are not well characterized and can only be detected by the ProteinChip system. As the ProteinChip system is not routinely available in clinical practice, we thought it would be necessary to identify a marker that could be monitored easily. In this study, SAA was identified as a candidate marker for PIR. Furthermore, this study showed the feasibility of quantitative analysis by the ProteinChip system, although the ProteinChip system has previously been considered to be a tool for semiquantitative analysis.

Serum biomarkers associated with leukemia[14] and cancer[15–21] have also been identified by the SELDI

ProteinChip technique. In some of these studies, SAA has been reported to be a potential marker for particular cancer status. Multiple variants of SAA have been detected by the SELDI ProteinChip technique in renal cancer patients.[20] The SELDI ProteinChip technique revealed that SAA may be a biomarker for identifying prostate cancer patients with bone lesions, with a sensitivity and specificity of 89.5%.[21]

SAA activates human mast cells, which leads to the degradation of SAA and the generation of an amyloidogenic SAA fragment.[22] SAA is a major acute-phase reactant that increases by as much as 1000-fold during inflammation. SAA is potentially involved in the pathogenesis of several chronic inflammatory diseases: it is the precursor of amyloid A protein deposited in amyloid A amyloidosis, and has also been implicated in the pathogenesis of atherosclerosis and rheumatoid arthritis.[23,24] SAA may be closely related to poor patient outcomes, including left ventricular systolic dysfunction, cardiac rupture and mortality in acute myocardial infarction.[25,26]

Some studies have suggested that the elevation of SAA may be associated with acute allograft rejection of the kidney,[27–30] liver[31] and heart.[32] By contrast, it has also been reported that SAA is inadequate for predicting acute rejection in cardiac allograft.[33] With regard to renal allograft rejection, SAA was shown to be a sensitive marker that rose above 100 mg/l in all cases of rejection, whereas C-reactive protein (CRP) showed little or no response to rejection.[29] We could not confirm whether or not the elevation of SAA was a phenomenon that occurs with all CBT around day 9, as the value of SAA in samples from non-febrile patients at this time point was not analyzed. However, it is unlikely that the elevation of SAA occurs with all allogeneic transplantation, as the phenomenon was not prominent in patients with acute GVHD. The possibility that the elevation of SAA was only a consequence of acute phase change that occurs with high-grade fever could not be completely ruled out, as the elevation of SAA was not confined to CBT; however, the elevation level was higher in PIR than in other conditions. Furthermore, patients who developed graft rejection had markedly higher levels of SAA. Although the reason for these observations is unclear, a previous report on SAA as an indication of allograft rejection has suggested that inflammation and cytokine production induced by an alloreaction may be related to the elevation of SAA in PIR.

In the case of CBT, SAA that increases in relation to PIR, as a factor associated with a poor prognosis of CBT, may be related to allograft rejection. Our retrospective study showed that pre-engraftment CRP values may predict acute GVHD and nonrelapse mortality.[34] Although CRP elevation was also observed during PIR, SAA elevation was more rapid and prominent. The SAA level was above the normal limit in all 13 samples at the day of fever onset, whereas 2 samples were within the normal limit for CRP. The mean SAA level was 121 times the upper normal limit at day 2 of fever onset, whereas the mean CRP level was 10 times the upper normal limit at the same time. SAA or anaphylatoxin C4a alone may lack specificity as a marker for PIR. However, the further analysis of samples obtained from CBT recipients by our method may provide fingerprints of markers useful for the diagnosis of PIR. Identification of peak markers suggests that the SELDI-TOF MS system in combination with other proteomic methods could serve as a potential diagnostic tool in discovering biomarkers for PIR after CBT.

Conflict of interest

The authors declare no conflict of interest.

Acknowledgements

This work was supported in part by grants from the Ministry of Health, Labor and Welfare, Japan.

References

1 Kishi Y, Kami M, Miyakoshi S, Kanda Y, Murashige N, Teshima T *et al.* Early immune reaction after reduced-intensity cord-blood transplantation for adult patients. *Transplantation* 2005; **80**: 34–40.
2 Miyakoshi S, Yuji K, Kami M, Kusumi E, Kishi Y, Kobayashi K *et al.* Successful engraftment after reduced-intensity umbilical cord blood transplantation for adult patients with advanced hematological diseases. *Clin Cancer Res* 2004; **10**: 3586–3592.
3 Uchida N, Wake A, Takagi S, Yamamoto H, Kato D, Matsuhashi Y *et al.* Umbilical cord blood transplantation after reduced-intensity conditioning for elderly patients with hematologic diseases. *Biol Blood Marrow Transplant* 2008; **14**: 583–590.
4 Takahashi S, Iseki T, Ooi J, Tomonari A, Takasugi K, Shimohakamada Y *et al.* Single-institute comparative analysis of unrelated bone marrow transplantation and cord blood transplantation for adult patients with hematologic malignancies. *Blood* 2004; **104**: 3813–3820.
5 Narimatsu H, Terakura S, Matsuo K, Oba T, Uchida T, Iida H *et al.* Short-term methotrexate could reduce early immune reactions and improve outcomes in umbilical cord blood transplantation for adults. *Bone Marrow Transplant* 2007; **39**: 31–39.
6 Mori T, Aisa Y, Nakazato T, Yamazaki R, Shimizu T, Mihara A *et al.* Tacrolimus and methotrexate for the prophylaxis of graft-versus-host disease after unrelated donor cord blood transplantation for adult patients with hematologic malignancies. *Transplant Proc* 2007; **39**: 1615–1619.
7 Heike Y, Hosokawa M, Osumi S, Fujii D, Aogi K, Takigawa N *et al.* Identification of serum proteins related to adverse effects induced by docetaxel infusion from protein expression profiles of serum using SELDI ProteinChip system. *Anticancer Res* 2005; **25**: 1197–1203.
8 Srinivasan R, Daniels J, Fusaro V, Lundqvist A, Killian JK, Geho D *et al.* Accurate diagnosis of acute graft-versus-host disease using serum proteomic pattern analysis. *Exp Hematol* 2006; **34**: 796–801.
9 Weissinger EM, Mischak H, Ganser A, Hertenstein B. Value of proteomics applied to the follow-up in stem cell transplantation. *Ann Hematol* 2006; **85**: 205–211.
10 Kaiser T, Kamal H, Rank A, Kolb HJ, Holler E, Ganser A *et al.* Proteomics applied to the clinical follow-up of patients after allogeneic hematopoietic stem cell transplantation. *Blood* 2004; **104**: 340–349.

11 Weissinger EM, Schiffer E, Hertenstein B, Ferrara JL, Holler E, Stadler M *et al.* Proteomic patterns predict acute graft-versus-host disease after allogeneic hematopoietic stem cell transplantation. *Blood* 2007; **109**: 5511–5519.
12 El Essawy B, Otu HH, Choy B, Zheng XX, Libermann TA, Strom TB. Proteomic analysis of the allograft response. *Transplantation* 2006; **82**: 267–274.
13 Yamayoshi Y, Watanabe T, Tanabe M, Hoshino K, Matsumoto K, Morikawa Y *et al.* Novel application of ProteinChip technology exploring acute rejection markers of rat small bowel transplantation. *Transplantation* 2006; **82**: 320–326.
14 Albitar M, Potts SJ, Giles FJ, O'Brien S, Keating M, Thomas D *et al.* Proteomic-based prediction of clinical behavior in adult acute lymphoblastic leukemia. *Cancer* 2006; **106**: 1587–1594.
15 Koopmann J, Zhang Z, White N, Rosenzweig J, Fedarko N, Jagannath S *et al.* Serum diagnosis of pancreatic adenocarcinoma using surface-enhanced laser desorption and ionization mass spectrometry. *Clin Cancer Res* 2004; **10**: 860–868.
16 Wong YF, Cheung TH, Lo KW, Wang VW, Chan CS, Ng TB *et al.* Protein profiling of cervical cancer by protein-biochips: proteomic scoring to discriminate cervical cancer from normal cervix. *Cancer Lett* 2004; **211**: 227–234.
17 Yang SY, Xiao XY, Zhang WG, Zhang LJ, Zhang W, Zhou B *et al.* Application of serum SELDI proteomic patterns in diagnosis of lung cancer. *BMC Cancer* 2005; **5**: 83.
18 Ward DG, Suggett N, Cheng Y, Wei W, Johnson H, Billingham LJ *et al.* Identification of serum biomarkers for colon cancer by proteomic analysis. *Br J Cancer* 2006; **94**: 1898–1905.
19 Malik G, Ward MD, Gupta SK, Trosset MW, Grizzle WE, Adam BL *et al.* Serum levels of an isoform of apolipoprotein A-II as a potential marker for prostate cancer. *Clin Cancer Res* 2005; **11**: 1073–1085.
20 Tolson J, Bogumil R, Brunst E, Beck H, Elsner R, Humeny A *et al.* Serum protein profiling by SELDI mass spectrometry: detection of multiple variants of serum amyloid alpha in renal cancer patients. *Lab Invest* 2004; **84**: 845–856.
21 Le L, Chi K, Tyldesley S, Flibotte S, Diamond DL, Kuzyk MA *et al.* Identification of serum amyloid A as a biomarker to distinguish prostate cancer patients with bone lesions. *Clin Chem* 2005; **51**: 695–707.
22 Niemi K, Baumann MH, Kovanen PT, Eklund KK. Serum amyloid A (SAA) activates human mast cells which leads into degradation of SAA and generation of an amyloidogenic SAA fragment. *Biochim Biophys Acta* 2006; **1762**: 424–430.
23 Uhlar CM, Whitehead AS. Serum amyloid A, the major vertebrate acute-phase reactant. *Eur J Biochem* 1999; **265**: 501–523.
24 Salazar A, Pinto X, Mana J. Serum amyloid A and high-density lipoprotein cholesterol: serum markers of inflammation in sarcoidosis and other systemic disorders. *Eur J Clin Invest* 2001; **31**: 1070–1077.
25 Katayama T, Nakashima H, Takagi C, Honda Y, Suzuki S, Iwasaki Y *et al.* Serum amyloid a protein as a predictor of cardiac rupture in acute myocardial infarction patients following primary coronary angioplasty. *Circ J* 2006; **70**: 530–535.
26 Katayama T, Nakashima H, Honda Y, Suzuki S, Yamamoto T, Iwasaki Y *et al.* The relationship between acute phase serum amyloid A (SAA) protein concentrations and left ventricular systolic function in acute myocardial infarction patients treated with primary coronary angioplasty. *Int Heart J* 2007; **48**: 45–55.
27 Muller TF, Trosch F, Ebel H, Grussner RW, Feiber H, Goke B *et al.* Pancreas-specific protein (PASP), serum amyloid A (SAA), and neopterin (NEOP) in the diagnosis of rejection after simultaneous pancreas and kidney transplantation. *Transpl Int* 1997; **10**: 185–191.
28 Maury CP, Teppo AM, Ahonen J, von Willebrand E. Measurement of serum amyloid A protein concentrations as test of renal allograft rejection in patients with initially non-functioning grafts. *Br Med J (Clin Res Ed)* 1984; **288**: 360–361.
29 Hartmann A, Eide TC, Fauchald P, Bentdal O, Herbert J, Gallimore JR *et al.* Serum amyloid A protein is a clinically useful indicator of acute renal allograft rejection. *Nephrol Dial Transplant* 1997; **12**: 161–166.
30 Fukuda Y, Hoshino S, Tanaka I, Yoneya T, Takeshita T, Sumimoto R *et al.* Examination of serum amyloid A protein in kidney transplant patients. *Transplant Proc* 2000; **32**: 1796–1798.
31 Feussner G, Stech C, Dobmeyer J, Schaefer H, Otto G, Ziegler R. Serum amyloid A protein (SAA): a marker for liver allograft rejection in humans. *Clin Investig* 1994; **72**: 1007–1011.
32 Muller TF, Vogl M, Neumann MC, Lange H, Grimm M, Muller MM. Noninvasive monitoring using serum amyloid A and serum neopterin in cardiac transplantation. *Clin Chim Acta* 1998; **276**: 63–74.
33 Vermes E, Kirsch M, Farrokhi T, Loisance D, Fanen P, Zimmermann R. Serum amyloid A protein: not a relevant marker for recognition of cardiac allograft rejection. *Transplantation* 2004; **78**: 950–951.
34 Fuji S, Kim SW, Fukuda T, Mori S, Yamasaki S, Morita-Hoshi Y *et al.* Preengraftment serum C-reactive protein (CRP) value may predict acute graft-versus-host disease and nonrelapse mortality after allogeneic hematopoietic stem cell transplantation. *Biol Blood Marrow Transplant* 2008; **14**: 510–517.

Published OnlineFirst September 30, 2013; DOI: 10.1158/1078-0432.CCR-13-0742

Cancer Therapy: Preclinical

Clinical Cancer Research

A Genetically Engineered Oncolytic Adenovirus Decoys and Lethally Traps Quiescent Cancer Stem-like Cells in S/G_2/M Phases

Shuya Yano[1], Hiroshi Tazawa[2], Yuuri Hashimoto[1], Yasuhiro Shirakawa[1], Shinji Kuroda[1], Masahiko Nishizaki[1], Hiroyuki Kishimoto[1], Futoshi Uno[1], Takeshi Nagasaka[1], Yasuo Urata[3], Shunsuke Kagawa[1], Robert M. Hoffman[4,5], and Toshiyoshi Fujiwara[1]

Abstract

Purpose: Because chemoradiotherapy selectively targets proliferating cancer cells, quiescent cancer stem-like cells are resistant. Mobilization of the cell cycle in quiescent leukemia stem cells sensitizes them to cell death signals. However, it is unclear that mobilization of the cell cycle can eliminate quiescent cancer stem-like cells in solid cancers. Thus, we explored the use of a genetically-engineered telomerase-specific oncolytic adenovirus, OBP-301, to mobilize the cell cycle and kill quiescent cancer stem-like cells.

Experimental Design: We established $CD133^+$ cancer stem-like cells from human gastric cancer MKN45 and MKN7 cells. We investigated the efficacy of OBP-301 against quiescent cancer stem-like cells. We visualized the treatment dynamics of OBP-301 killing of quiescent cancer stem-like cells in dormant tumor spheres and xenografts using a fluorescent ubiquitination cell-cycle indicator (FUCCI).

Results: $CD133^+$ gastric cancer cells had stemness properties. OBP-301 efficiently killed $CD133^+$ cancer stem-like cells resistant to chemoradiotherapy. OBP-301 induced cell-cycle mobilization from G_0–G_1 to S/G_2/M phases and subsequent cell death in quiescent $CD133^+$ cancer stem-like cells by mobilizing cell-cycle–related proteins. FUCCI enabled visualization of quiescent $CD133^+$ cancer stem-like cells and proliferating $CD133^-$ non-cancer stem-like cells. Three-dimensional visualization of the cell-cycle behavior in tumor spheres showed that $CD133^+$ cancer stem-like cells maintained stemness by remaining in G_0–G_1 phase. We showed that OBP-301 mobilized quiescent cancer stem-like cells in tumor spheres and xenografts into S/G_2/M phases where they lost viability and cancer stem-like cell properties and became chemosensitive.

Conclusion: Oncolytic adenoviral infection is an effective mechanism of cancer cell killing in solid cancer and can be a new therapeutic paradigm to eliminate quiescent cancer stem-like cells. *Clin Cancer Res; 19(23); 6495–505. ©2013 AACR.*

Introduction

Current cytotoxic chemoradiotherapy selectively targets proliferating cancer cells. Quiescent or dormant cancer cells in contrast are often drug-resistant and are a major impediment to cancer therapy (1, 2). Cancer stem-like cells or tumor-initiating cells (3–5) maintain a quiescent or dormant state, which appears to contribute to their resistance to conventional therapies (6–8). Recently, several therapeutic strategies have targeted inhibition of the cancer stem-like cell quiescent state. For example, treatment with arsenic trioxide enhanced the sensitivity of leukemia stem cells (LSC) to cytosine arabinoside through inhibition of LCS quiescence (9). Acute myeloid leukemia stem cells can be induced to enter the cell cycle and apoptosis by treatment with granulocyte colony-stimulating factor (10). However, it is still unclear whether cancer stem-like cells in solid tumors can also be eliminated by inducing them to cycle.

Viruses can infect target cells, multiply, cause cell death, and release viral particles. These features enable the use of viruses as anticancer agents that induce specific tumor lysis (11, 12). Adenoviral E1A, in particular, has been shown to exert tumor-suppressive functions, including enhancement of chemoradiotherapy-induced apoptosis via inhibition of the cellular DNA repair machinery (13)

Authors' Affiliations: [1]Department of Gastroenterological Surgery, Okayama University Graduate School of Medicine, Dentistry and Pharmaceutical Sciences; [2]Center for innovative clinical medicine, Okayama University Hospital, Okayama; [3]Oncolys BioPharma, Inc., Tokyo, Japan; [4]Department of Surgery, University of California San Diego; and [5]AntiCancer, Inc., San Diego, California

Note: Supplementary data for this article are available at Clinical Cancer Research Online (http://clincancerres.aacrjournals.org/).

Corresponding Author: Toshiyoshi Fujiwara, Department of Gastroenterological Surgery, Okayama University Graduate School of Medicine, Dentistry, and Pharmaceutical Sciences, 2-5-1 Shikata-cho, Kita-ku, Okayama 700-8558, Japan. Phone: 81-86-235-7255; Fax: 81-86-221-8775; E-mail: toshi_f@md.okayama-u.ac.jp

doi: 10.1158/1078-0432.CCR-13-0742

Published OnlineFirst September 30, 2013; DOI: 10.1158/1078-0432.CCR-13-0742

Translational Relevance

Current chemotherapy and radiotherapy target proliferating cancer cells, while having little effect on dormant cancer cells. Cancer stem–like cells can maintain a quiescent or dormant state, which contributes largely to their resistance to conventional therapies. Recently, several therapeutic strategies have targeted inhibition of the quiescent state in leukemia stem cells. However, it is still unclear whether cancer stem–like cells in solid tumors can also be eliminated by inhibition of their dormant state. Here, we show that a telomerase-specific adenovirus, OBP-301, mobilizes quiescent cancer stem–like cells to cycle and lethally traps them into S-phase. Moreover, we showed by spatiotemporal treatment dynamics that OBP-301 decoyed quiescent cancer stem–like cells in tumor spheres and xenografts into an S-phase trap where they lost viability and cancer stem–like cell properties and become chemosensitive. Thus, our data demonstrated that cell-cycle mobilization and $S/G_2/M$ phase trapping induced by adenoviral infection is an effective mechanism of killing cancer stem–like cells in solid cancers.

and inhibition of cell proliferation via suppression of EGH receptor (EGFR; ref. 14) and HER-2 (15). It has been recently reported that an oncolytic adenovirus efficiently eradicates cancer stem–like cells as well as non–cancer stem–like cells in brain tumors, breast cancer, and esophageal cancer (16–18).

In the present study, we isolated $CD133^+$ subpopulations from radioresistant cells in human gastric cancer cell lines and characterized them as cancer stem–like cells. By using multicolor cell-cycle imaging that color codes the quiescent cancer stem–like cells and proliferating non–cancer stem–like cells, we showed by treatment dynamics that a genetically engineered telomerase-specific oncolytic adenovirus, OBP-301 (19, 20), eradicates dormant $CD133^+$ cancer stem–like cells via cell-cycle mobilization both in tumor spheres and in subcutaneous tumors.

Materials and Methods

Cell lines and radiation treatment

The human gastric cancer cell lines MKN45 and MKN7 were maintained according to the vendor's specifications (21). Radioresistant MKN45 and MKN7 cells were established by administration of radiation treatments using an X-ray generator (MBR-1505R; Hitachi Medical Co.).

Recombinant adenoviruses

The recombinant tumor-specific, replication-selective adenovirus vector OBP-301 (Telomelysin), in which the promoter element of the human telomerase reverse transcriptase (hTERT) gene drives the expression of E1A and E1B genes linked to an internal ribosome entry site, was previously constructed and characterized (19, 22).

Isolation of $CD133^+$ and $CD133^-$ cells by flow cytometry

After incubation with an anti-CD133/2(293C)-allophycocyanin antibody (Miltenyi Biotec), $CD133^+$ cells were sorted by flow cytometry using a FACSAria flow cytometer (Becton Dickinson). $CD133^+$ and $CD133^-$ cells were separated by flow cytometry just before each experiment to ensure that the purity of the $CD133^+$ population was greater than 70%, and the purity of $CD133^-$ cells was above 99%.

Cell viability assay

$CD133^+$ and $CD133^-$ cells (5×10^2 cells/well) in 96-well plates were treated with OBP-301, cisplatin, or radiation at the indicated doses. Cell viability was determined on day 5 after treatment using the Cell Proliferation Kit II (Roche Molecular) according to the manufacturer's protocol.

Establishment of MKN45 cells stably transfected with FUCCI vector plasmids

FUCCI (fluorescent ubiquitination-based cell-cycle indicator) (23) was used to visualize the cell-cycle phases. Plasmids, expressing mKO2-hCdt1 (GFP) or mAG-hGem (orange fluorescence protein), were obtained from the Medical & Biological Laboratory. Plasmids expressing mKO2-hCdt1 or mAG-hGem were transfected into radioresistant MKN45 cells using Lipofectamine LTX (Invitrogen).

Western blot analysis

The primary antibodies used were: mouse anti-CD133/1(W6B3C) monoclonal antibody (mAb; Miltenyi Biotec); rabbit anti-E2F1 polyclonal antibody (pAb) (Santa Cruz Biotechnology); mouse anti-Ad5 E1A mAb (BD Pharmingen); mouse anti-c-Myc pAb, rabbit anti-phospho-Akt mAb, rabbit anti-Akt mAb, mouse anti-p27 mAb (all from Cell Signaling Technology); mouse anti-p53 mAb, mouse anti-p21 mAb (both from CALBIOCHEM Merck4 Biosciences); and mouse anti-β-actin mAb (Sigma-Aldrich). Immunoreactive bands on the blots were visualized using enhanced chemiluminescence substrates (ECL Plus; GE Healthcare).

Subcutaneous MKN45 tumor xenograft model

To evaluate a tumorigenicity of $CD133^+$ and $CD133^-$ cells, purified $CD133^+$ and $CD133^-$ cells from radioresistant MKN45 were inoculated at a density of 1×10^5 cells/site on the right and left sides, respectively, of the flank of 5-week-old female NOD/SCID mice (Charles River Laboratories) or athymic nude mice (Charles River Laboratories). To evaluate the *in vivo* antitumor efficacy of OBP-301, cisplatin, or radiation, the radioresistant MKN45 cells were inoculated at a density of 5×10^6 cells/site into the flank of 5-week-old female athymic nude mice. OBP-301 [1×10^8 plaque-forming units (PFU)] was injected into the tumors. Cisplatin (4 mg/kg body weight) was intraperitoneally injected and ionizing radiation (2 Gy) was administered to tumors after protection of normal tissues. Mice were treated every 3 days for a total of three treatments.

Published OnlineFirst September 30, 2013; DOI: 10.1158/1078-0432.CCR-13-0742

Imaging of MKN45 cells expressing cell-cycle–dependent fluorescent proteins

Time lapse images of FUCCI-expressing CD133$^+$ and CD133$^-$ radioresistant MKN45 cells were acquired using a confocal laser scanning microscope (FV10i; Olympus). Cross-sections of FUCCI-expressing tumors were imaged using a confocal laser scanning microscope (FV-1000; Olympus).

Treatment of subcutaneous FUCCI-expressing MKN45 tumors

To evaluate the *in vivo* antitumor efficacy of OBP-301, cisplatin, paclitaxel, or their combination, the FUCCI-expressing MKN45 cells were inoculated at a density of 5×10^6 cells/site into the flank of 5-week-old female athymic nude mice (Charles River Laboratories). OBP-301 (1×10^8 PFU/tumor) was injected into the tumors. Cisplatin (4 mg/kg) and paclitaxel (5 mg/kg) were injected intraperitoneally. Mice were treated every 3 days for a total of 3 to 5 treatments.

Statistical analysis

Data are shown as means ± SD. For comparison between 2 groups, significant differences were determined using the Student *t* test. For comparison of more than 2 groups, statistical significance was determined with a one-way ANOVA followed by a Bonferroni multiple-group comparison test. $P < 0.05$ was considered significant.

Results

CD133$^+$ cells in human gastric cancer cells are cancer stem–like

Cancer stem–like cells are more resistant to radiotherapy than non–cancer stem–like cells (24–26). To enrich cancer stem–like subpopulations, we established radioresistant MKN45 and MKN7 human gastric cancer cells. Radioresistant MKN45 and MKN7 cells had a significantly higher percentage of CD133$^+$ cells than parental cells (Fig. 1A and Supplementary Fig. S1A). We hypothesized that CD133 in gastric cancer would identify cancer cells with stem-like properties, such as asymmetric cell division, *in vitro* proliferation, dormancy, sphere formation, and *in vivo* tumorigenicity (5, 6). To investigate the asymmetric division of CD133$^+$ cells, we determined whether CD133$^+$ cells produce both CD133$^+$ and CD133$^-$ cells. CD133$^+$ cells generated both CD133$^+$ and CD133$^-$ cells, whereas CD133$^-$ cells could not produce CD133$^+$ cells (Supplementary Fig. S2). We compared *in vitro* proliferation of CD133$^+$ and CD133$^-$ cells. CD133$^+$ cells produced larger colonies than CD133$^-$ cells (Fig. 1B and Supplementary Fig. S3). CD133$^+$ cells made significantly much more tumor spheres than CD133$^-$ cells (Fig. 1B). CD133$^+$ cells produced tumors in immunodeficient nude mice and NOD/SCID mice, whereas CD133$^-$ cells did not generate tumors in either nude on NOD/SCID mice (Supplementary Fig. S4 and Fig. 1B). Furthermore, CD133$^+$ cells in radioresistant MKN45 and MKN7 cells were significantly more resistant to 5-fluorouracil, cisplatin, paclitaxel, and radiation than CD133$^-$ cells (Fig. 1C and Supplementary Fig. S1B). These data indicate that CD133$^+$ cells are cancer stem–like.

Quiescent CD133$^+$ cancer stem–like cells and cycling CD133$^-$ non–cancer stem–like cells are independently visualized by fluorescent cell-cycle indicator technology

Sakaue-Sawano and colleagues have reported that the cell-cycle state in viable cells can be visualized using the FUCCI system (23). We established FUCCI-expressing CD133$^+$ or CD133$^-$ radioresistant MKN45 cells, in which cell nuclei in G_0–G_1, S, or G_2–M phases exhibit red, yellow, or green fluorescence, respectively. We compared the cell-cycle phase of FUCCI-expressing CD133$^+$ or CD133$^-$ cells. Time-lapse imaging showed that most of CD133$^+$ cells were quiescent in G_0–G_1 phase with red fluorescent nuclei compared with CD133$^-$ cells (Fig. 1D). Similar results were also observed in flow cytometric analysis of the cell cycle (Supplementary Fig. S5A and S5B). CD133$^+$ cells had similar proliferation rates as CD133$^-$ cells until 3 days after seeding. CD133$^+$ cells showed lower proliferation rates than CD133$^-$ cells 5 days after seeding (Fig. 1D). This result was consistent with the cell-cycle status of CD133$^+$ cells which had an increased percentage of cells in G_0–G_1 phase. Moreover, we examined cell-cycle–related protein (27) expression in CD133$^+$ and CD133$^-$ cells. CD133$^+$ cells showed higher expressions of p53, p21, and p27 proteins compared with CD133$^-$ cells (Supplementary Fig. S8), suggesting that these proteins are involved in the maintenance of quiescent cancer stem–like cells.

OBP-301 efficiently kills cancer stem–like cells and reduces cancer stem–like cell frequency via enhanced viral replication

To evaluate the efficacy of OBP-301 against CD133$^+$ cancer stem–like cells, we treated CD133$^+$ and CD133$^-$ cells from radioresistant MKN45 and MKN7 cells with OBP-301. OBP-301 similarly killed CD133$^+$ and CD133$^-$ cells (Fig. 2A and Supplementary Fig. S1B). Next we investigated whether OBP-301 could decrease cancer stem–like cell frequency. Flow cytometric analysis showed that OBP-301 significantly decreased the percentage of CD133$^+$ cells compared with cisplatin or radiation (Fig. 2A). Expression of *CD133* mRNA was closely associated with the population of CD133$^+$ cells (Supplementary Fig. S6). OBP-301 significantly suppressed the expression of *CD133* mRNA compared with cisplatin and radiation (Supplementary Fig. S7). Western blot analysis also showed that cisplatin and radiation, but not OBP-301, increased CD133 expression 3- to 5-fold in CD133$^+$ cells (Fig. 2D). Moreover, pretreatment of CD133$^+$ cells with OBP-301, but not cisplatin or radiation, significantly decreased the number of tumor spheres (Supplementary Fig. S13). These data indicated that OBP-301 kills both CD133$^+$ and CD133$^-$ cells and reduces cancer stem–like cell frequency.

To further explore the efficacy of OBP-301 against CD133$^+$ cancer stem–like cells, we assessed the relationship between hTERT activity and viral replication. OBP-301 contains the hTERT promoter, which allows it to tumor-specifically regulate the gene expression of E1A and E1B for viral replication (19). Quantitative reverse transcription

Published OnlineFirst September 30, 2013; DOI: 10.1158/1078-0432.CCR-13-0742

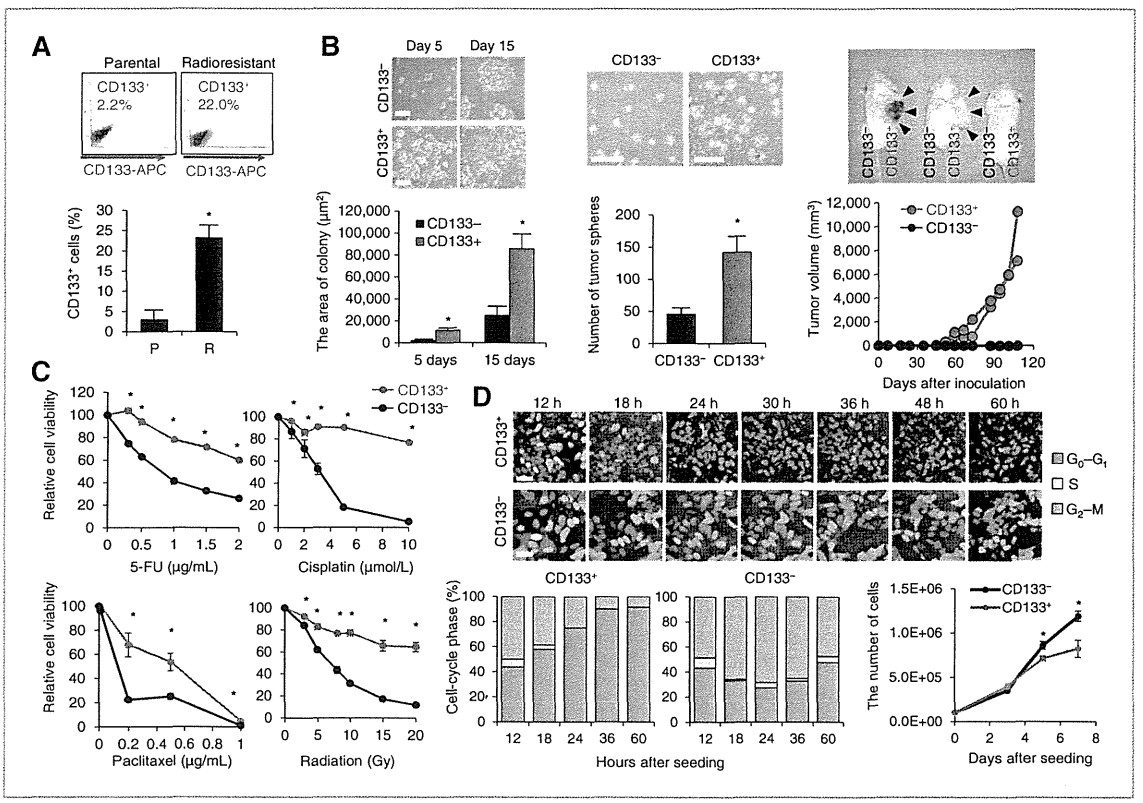

Figure 1. CD133$^+$ cancer stem–like cells in human gastric cancer exhibit cancer stem–like cell properties and are more quiescent. A, flow cytometric analysis of CD133 expression in parental (P) and radioresistant (R) MKN45 cells. Representative dot plots (top) and data from 5 experiments (bottom) are shown. B, CD133$^+$ MKN45 cancer cells exhibit cancer stem–like properties. Representative images of colonies from CD133$^+$ or CD133$^-$ cells. Histogram shows the size of colonies from CD133$^+$ or CD133$^-$ cells (left). Quantitative measurement of the tumor sphere–forming potential of CD133$^+$ and CD133$^-$ cells (middle). Representative images of tumor spheres derived from CD133$^+$ and CD133$^-$ cells. Histogram shows the numbers of tumor spheres from CD133$^+$ or CD133$^-$ cells. Scale bars, 500 μm. Tumorigenicity of CD133$^+$ and CD133$^-$ cells in immunodeficient NOD/SCID mice (right). Growth curve of each tumor and representative photographs are shown. C, sensitivity of CD133$^+$ and CD133$^-$ cells from radioresistant MKN45 cells to 5-fluorouracil, cisplatin, paclitaxel, and irradiation. D, time-lapse imaging of CD133$^+$ and CD133$^-$ cells from radioresistant MKN45 cells expressing cell-cycle–dependent fluorescent proteins (FUCCI; top). The cells in G_0–G_1, S, or G_2–M phases appear red, yellow, or green, respectively. Histogram shows the cell-cycle phase of FUCCI-expressing CD133$^+$ and CD133$^-$ cells cultured for 48 hours after sorting (bottom left). The percentage of cells in G_0–G_1, S, and G_2–M phases are shown. Cell proliferation rate of CD133$^+$ and CD133$^-$ cells (bottom right). Scale bars, 50 μm. Data are shown as means ± SD ($n = 5$). *, $P < 0.01$.

PCR (qRT-PCR) showed that CD133$^+$ cells had a significant, 3-fold higher expression of *hTERT* mRNA than CD133$^-$ cells (Fig. 2B), suggesting that CD133$^+$ cancer stem–like cells have a higher activity of hTERT than CD133$^-$ cells. Next we compared the expression of *E1A* mRNA and E1A protein in CD133$^+$ cells and in CD133$^-$ cells. qRT-PCR showed that the expression of *E1A* mRNA in CD133$^+$ cells was higher than that in CD133$^-$ cells (Fig. 2B). Western blotting showed that the expression of E1A in CD133$^+$ cells was higher than that in CD133$^-$ cells (Fig. 2B). Furthermore, we compared the copy number of the E1A gene, which is indicative of viral replication, in CD133$^+$ and CD133$^-$ cells after infection with OBP-301. As expected, the copy number of the E1A gene in CD133$^+$ cells was significantly higher than that in CD133$^-$ cells (Fig. 2B). These data indicate that OBP-301 is efficiently cytopathic for CD133$^+$ cells due to enhanced viral replication.

OBP-301 mobilizes and lethally traps quiescent cancer stem–like cells into S-phase in monolayer culture

To examine whether OBP-301 could change the cell-cycle phase of quiescent CD133$^+$ cells, we treated FUCCI-expressing CD133$^+$ cells with OBP-301. Time-lapse imaging showed that OBP-301 infection significantly decreased the percentage of CD133$^+$ cells in G_0–G_1 phase, increased the percentage of CD133$^+$ cells in S-phase, and killed them in S-phase (Fig. 2C and Supplementary Movie S1). Similar results were also observed in flow cytometric analysis of the cell cycle (Supplementary Fig. S5C and S5D). These results suggest that OBP-301 induces cell-cycle activation of quiescent CD133$^+$ cells from G_0–G_1 phase to S-phase and kills them. We next assessed the molecular mechanism by which OBP-301 induces mobilization of the cell cycle in quiescent cancer stem–like cells. OBP-301 increased the expression of E2F1, c-Myc, and phospho-Akt proteins that function as